Low dose of dopamine may stimulate prolactin secretion by increasing fast potassium currents

Joël Tabak · Natalia Toporikova · Marc E. Freeman · Richard Bertram

Abstract Dopamine (DA) released from the hypothalamus tonically inhibits pituitary lactotrophs. DA (at micromolar concentration) opens potassium channels, hyperpolarizing the lactotrophs and thus preventing the calcium influx that triggers prolactin hormone release. Surprisingly, at concentrations ∼1000 lower, DA can stimulate prolactin secretion. Here, we investigated whether an increase in a K^+ current could mediate this stimulatory effect. We considered the fast K^+ currents flowing through large-conductance BK channels and through A-type channels. We developed a minimal lactotroph model to investigate the effects of these two currents. Both I_{BK} and I_A could transform the electrical pattern of activity from spiking to bursting, but through distinct mechanisms. I_{BK} always increased the intracellular Ca^{2+} concentration, while I_A could either increase or decrease it. Thus, the stimulatory effects of DA could be mediated by a fast K^+ conductance which converts tonically spiking cells to bursters. In addition, the study illustrates that a heterogeneous distribution of fast K^+ conductances could cause heterogeneous lactotroph firing patterns.

Keywords Lactotrophs · Bursting · Calcium · Fast/slow analysis

Introduction

Release of prolactin (PRL) by pituitary lactotroph cells is under the inhibitory control of hypothalamic dopamine (DA) (Ben Jonathan and Hnasko, 2001). DA acts through the D2 receptor to decrease PRL synthesis and secretion. Secretion is decreased in part by hyperpolarizing the lactotroph membrane (Einhorn et al., 1991), which prevents action potentials and the associated increase in intracellular calcium concentration ([Ca]) that triggers exocytosis. This hyperpolarization is caused by activation of an inward rectifying potassium current (Gregerson et al., 2001; Oxford and Tse, 1993), and an A-type K^+ current is also increased by DA (Lledo et al., 1990b). *In vitro*, this inhibition occurs at DA concentrations around 0.1–10 μM.

Surprisingly, at a lower dose (sub-nanomolar concentrations, about 1000-fold lower than the inhibitory dose), DA has been shown to have a stimulatory effect on the release of PRL (Arey et al., 1993; Denef et al., 1980). The stimulatory effect is mediated, at least in part, through an increase in [Ca] (Burris and Freeman, 1993). However, no biophysical mechanism for this stimulatory action of DA has been identified. How can DA stimulate Ca^{2+} entry if it is increasing inhibitory K^+ currents?

It was shown recently that activation of the large-conductance calcium-activated K^+ current (BK) may increase hormone secretion by pituitary cells (Van Goor et al., 2001a). Although many pituitary cells spike spontaneously, if the spikes are too narrow they may allow only a small

Action Editor: Christiane Linster

J. Tabak (✉) · M. E. Freeman
Department of Biological Science, Florida State University, Tallahassee, FL, 32306
e-mail: joel@neuro.fsu.edu

M. E. Freeman
e-mail: freeman@neuro.fsu.edu

N. Toporikova · R. Bertram
Department of Mathematics, Florida State University, Tallahassee, FL, 32306

N. Toporikova
e-mail: ntoporik@math.fsu.edu

R. Bertram
e-mail: bertram@math.fsu.edu

amount of Ca^{2+} entry so the basal level of hormone secretion is low. The presence of BK channels in pituitary cells can broaden their spikes or even transform the spiking pattern into a bursting pattern. This transformation of the spike waveform could result in an increase in the Ca^{2+} entry into the cells, which in turn would increase hormone secretion. The effect of the BK current was explained in the following way. At the beginning of an action potential, the associated Ca^{2+} flux rapidly activates the BK channels. This activation is very brief, stopping as soon as the associated Ca^{2+} channel closes, since the BK channel responds to the high-concentration Ca^{2+} microdomain at the mouth of an open channel (Prakriya and Lingle, 2000; Roberts et al., 1990). This quick and brief K^+ current reduces the amplitude of the action potential, thus reducing the activation of the delayed rectifier (DR) K^+ channels that are primarily responsible for terminating the action potential. Because the DR current is reduced, the spikes are broader. The reduced DR current also results in a blunted repolarization after the spike, so in some cases a burst of spikes occurs before a complete repolarization of the membrane (Van Goor et al., 2001a).

The work of Van Goor et al. (2001a) motivated us to consider if the addition of fast K^+ currents can be responsible for the stimulatory effect of DA in lactotrophs. This effect could be mediated by increasing BK channels, which are present in lactotrophs (Van Goor et al., 2001c) and are activated by DA (Kanyicska et al., 1997). Another current whose conductance is increased by DA is the fast, inactivating A-type K^+ channel (Liu et al., 1994; Lledo et al., 1990b). We asked (1) whether the addition of such currents could transform the spiking pattern and increase Ca^{2+} influx in lactotrophs and, if so, (2) whether these two currents would operate through the same mechanism.

To obtain a clear understanding of the postulated DA effects, we use a minimal model of the lactotroph. This model has the right set of currents to generate bursting, but the parameters are chosen so that it operates in a spiking mode. We added either a BK-type current (modeled simply as a fast voltage-gated K^+ channel) or an A-type current (fast, voltage-gated, with inactivation) to this minimal model. We found that the addition of either type of current could transform the spiking into a bursting pattern, but the effect on cytosolic Ca^{2+} concentration was dependent on the type of current. Specifically, increasing the BK-like current reliably increased [Ca], while increasing the A-current could lead to either an increase or a decrease in [Ca], depending on model parameters. To explain these differences, we perform a phase plane analysis of the model with either added K^+ current. The analysis demonstrates that the BK-like and A-type currents transform spiking into bursting through distinct mechanisms. Furthermore, the A-type K^+ current can transform the spike pattern into bursting even in the absence of the classical ingredients for bursting—bistability between a spiking and a silent state, plus a slow process to switch between states.

Model

The basic lactotroph model incorporates three voltage-gated currents. A Ca^{2+} current (I_{Ca}) and a delayed-rectifier K^+ current (I_K) constitute the spike-generating mechanism. Like other pituitary cells, Ca^{2+} provides the upstroke for action potentials in lactotrophs, although Na^+ currents may also play a role (Horta et al., 1991). A slow, Ca^{2+}-activated K^+ current (I_{SK}) provides the burst-generation mechanism (Chay and Keizer, 1983). Activity-dependent activation of I_{SK} can terminate a burst, and deactivation of the current can start a new burst. However, in this study we have chosen a set of parameters such that the model lactotroph is spiking, not bursting, if no additional currents are added. The equations of the lactotroph model describe the dynamics of the three variables V (membrane potential), n (activation of I_K) and [Ca] (intracellular Ca^{2+} concentration):

$$C\frac{dV}{dt} = -(I_{Ca} + I_K + I_{SK}) \tag{1}$$

$$\tau_n\frac{dn}{dt} = \lambda(n_\infty(V) - n) \tag{2}$$

$$\frac{d[Ca]}{dt} = -f_c(\alpha I_{Ca} + k_c[Ca]) \tag{3}$$

with

$$I_{Ca} = g_{Ca}\,m_\infty(V)(V - V_{Ca}) \text{ and}$$

$$m_\infty(V) = [1 + \exp((v_m - V)/s_m)]^{-1}$$

$$I_K = g_K\,n(V - V_K) \text{ and}$$

$$n_\infty(V) = [1 + \exp((v_n - V)/s_n)]^{-1}$$

$$I_{SK} = g_{SK}\,s_\infty([Ca])(V - V_K) \text{ and}$$

$$s_\infty([Ca]) = \frac{[Ca]^2}{[Ca]^2 + k_s^2}$$

where m_∞, n_∞, s_∞, are steady state functions. We have assumed that the Ca^{2+} concentration is homogeneous so variations of [Ca] represent the balance between Ca^{2+} entry through I_{Ca} and extrusion through pumps and exchangers (Eq. (3)). The fraction of Ca^{2+} ions not bound to endogenous buffers, f_c, determines the time constant of [Ca] variations. Measurements of f_c in neurons and other cell types yield values around 0.01 (Helmchen et al., 1996; Neher and Augustine, 1992).

We hypothesized that a low dose of dopamine would increase a fast potassium current, $I_{K(DA)}$. For simplicity, the conductance associated with this current is null before addition of DA. Thus, in the presence of low DA, Eq. (1) becomes:

$$C\frac{dV}{dt} = -(I_{Ca} + I_K + I_{SK} + I_{K(DA)}) \tag{1}$$

with

$$I_{K(DA)} = I_{BK} = g_{BK}\, f_\infty(V - V_K) \text{ and}$$
$$f_\infty(V) = [1 + \exp((v_f - V)/s_f)]^{-1}$$

or

$$I_{K(DA)} = I_A = g_a\, a_\infty\, h(V - V_K) \text{ and}$$
$$a_\infty(V) = [1 + \exp((v_a - V)/s_a)]^{-1}$$

Although BK channels are also Ca-dependent, we ignored this dependency because the Ca^{2+} concentration in the domain sensed by the BK channels varies similarly to the membrane potential in the model of Van Goor et al. (2001a). In the case $I_{K(DA)} = I_A$, a fourth variable is added, the inactivation of the A-type K^+ current, h, described by the following equation

$$\tau_h \frac{dh}{dt} = h_\infty(V) - h \tag{4}$$

with $h_\infty(V) = [1 + \exp((v_h - V)/s_h)]^{-1}$

Finally, prolactin secretion rate is given by the dimensionless quantity

$$\text{PRL} = k_{PRL}[Ca]^4$$

where it is assumed that granule exocytosis is triggered by the binding of four Ca^{2+} ions as with synaptic transmitter release (Dodge and Rahamimoff, 1967).

Parameter definitions and values are given in Table 1. Values of the kinetic parameters for I_{Ca} were based on Lledo et al. (1990a) and the values for I_K and I_A were based on Herrington and Lingle (1994). The activation and inactivation curves for the voltage-dependent K^+ currents are shown in Fig. 1. Note that I_A is activated at the lowest voltages, but inactivates above -40 mV. Equations were integrated, and bifurcation diagrams were constructed, using the package XPPAUT (Ermentrout, 2002). The 4th-order Runge-Kutta integration method was used with a time step of 2 ms (decreasing the time step did not affect the simulation results). The code for this model is freely available at www.math.fsu.edu/~bertram/software/pituitary.

Table 1 Parameter values used in the simulations

Parameter	Value	Definition
C	10 pF	Membrane capacitance
g_{Ca}	2 nS	Maximal conductance of Ca channels
V_{Ca}	50 mV	Reversal potential for Ca^{2+}
v_m	-20 mV	Voltage value at midpoint of m_∞
s_m	12 mV	Slope parameter of m_∞
g_K	4 nS	Maximal conductance of K channels
V_K	-75 mV	Reversal potential for K^+
v_n	-5 mV	Voltage value at midpoint of n_∞
s_n	10 mV	Slope parameter of n_∞
τ_n	30 ms	Time constant of n
λ	0.7	Parameter used to control spiking pattern
g_{SK}	1.7 nS	Maximal conductance of SK channels
k_s	0.5 μM	[Ca] at midpoint of s_∞
g_{BK}	0–0.7 nS	Maximal conductance of BK channels
v_f	-20 mV	Voltage value at midpoint of f_∞
s_f	5.6 mV	Slope parameter of f_∞
g_A	0–40 nS	Maximal conductance of A channels
v_a	-20 mV	Voltage value at midpoint of a_∞
s_a	10 mV	Slope parameter of a_∞
v_h	-60 mV	Voltage value at midpoint of h_∞
s_h	5 mV	Slope parameter of h_∞
τ_h	20 ms	Time constant of h
f_c	0.01	Fraction of free Ca ions in cytoplasm
α	0.0015 μM fC^{-1}	Conversion from charges to molar concentration
k_c	0.1–0.16 ms^{-1}	Rate of Ca^{2+} extrusion
k_{PRL}	1 μM^{-4}	Dimensionality constant for PRL

Results

I_{BK} converts spiking to bursting and increases [Ca]

We first added I_{BK} to the spiking lactotroph model. Figure 2 illustrates the effects of increasing g_{BK} from 0 to 0.2 and 0.4 nS. For $g_{BK} = 0$ (A), the lactotroph is spiking so the basal [Ca] is elevated (with mean above 0.2 μM, which is higher than the Ca^{2+} level of the resting cell $\sim$0.05 μM). In this condition, the basal level of prolactin release is low. When g_{BK} is increased to 0.2 nS (B), there is little effect on spike frequency and spike duration, but [Ca] is slightly increased, resulting in a small increase in PRL secretion. Finally, if g_{BK} is increased to 0.4 nS, the firing pattern switches to bursting. This new pattern is characterized by a significantly increased cytosolic Ca^{2+} concentration and PRL secretion. Experimentally recorded lactotroph bursting patterns also show small amplitude spiking during the active phase and are slightly slower than bursting produced by our model (Van Goor et al., 2001b).
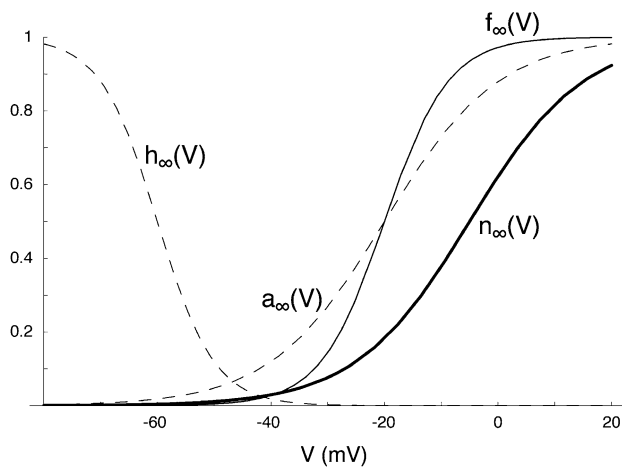
Fig. 1 Activation and inactivation functions of the voltage-dependent K$^+$ currents. Thick black curve: activation of I_K (n_∞). Thin curve: activation of I_{BK} (f_∞). Dashed curves: activation and inactivation of I_A (a_∞, h_∞). Both I_{BK} and I_A turn on at lower voltages than I_K

In the model of Van Goor et al. (2001a), the Ca^{2+} influx was minimal when the pituitary cell was spiking. I_{BK} increased [Ca] by broadening the spikes or by switching from a spiking to a bursting pattern. Here, however, basal [Ca] is already elevated (compared to rest) and is further increased by the transition to bursting. To better understand how, in our model, I_{BK} causes a transition from spiking to bursting and an accompanying increase in cytosolic Ca^{2+} concentration, we use a fast/slow analysis, shown in Fig. 3.

The two panels in Fig. 3(A) show bifurcation diagrams of the model for different values of g_{BK}. They are obtained by treating [Ca] as a parameter and determining the steady state and periodic solutions of the $V-n$ fast subsystem as a function of [Ca]. See Rinzel and Ermentrout (1998) for a detailed description of this fast/slow analysis technique. The z-shaped curve (or "z-curve") represents the steady states (thick: stable, thin: unstable) and the ε-shaped curve is the periodic branch, representing the minimum and maximum of the periodic oscillations (solid: stable, dashed: unstable) of V. Superimposed on each diagram is the Ca-nullcline (dashed-dotted line, defined by the points ([Ca], V) for which d[Ca]$/dt = 0$). Also superimposed is the trajectory of the full three-variable system projected onto the ([Ca], V) plane. The trajectories shown on the left and right panels of Fig. 3(A) correspond to the time courses of V and [Ca] from Fig. 2(A) and (C), respectively. These two trajectories are typical of spiking (left, trajectory mostly vertical with [Ca] varying little between the beginning and end of a spike) and bursting (right, with oscillations around the higher steady state and large variations of [Ca] between the beginning and end of a burst).

The main consequence of increasing g_{BK} from 0 (left panel) to 0.4 nS (right panel) is that the periodic branch has moved to the right, while the z-curve is almost unchanged. The large-amplitude spiking branch disappears and there is now a region of bistability between low and high stable steady states. The activity pattern is changed to bursting,
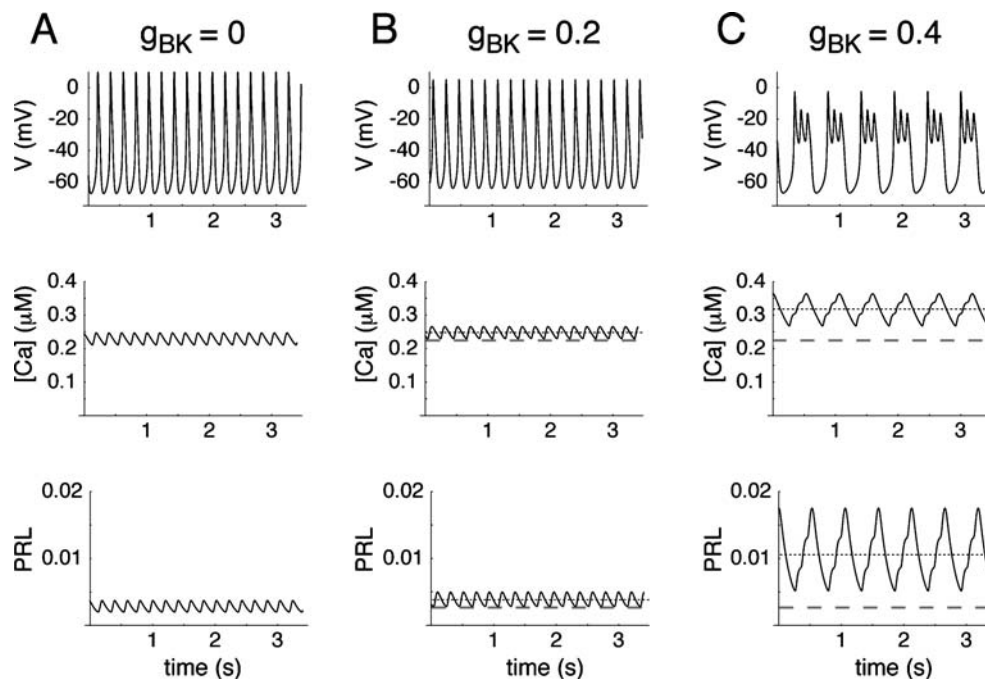
Fig. 2 Effect of I_{BK} on spike pattern, intracellular Ca^{2+} concentration and PRL release. For $g_{BK} = 0$ (A), the lactotroph model is spiking, [Ca] and PRL levels are above 0. Adding a small amount of BK conductance (B, $g_{BK} = 0.2$ nS) does not change the spike pattern but moderately increases [Ca] and PRL levels. These levels increase more significantly when the pattern switches to bursting (C, $g_{BK} = 0.4$ nS). In B and C, dotted lines represent the mean value, dashed lines represent mean value for $g_{BK} = 0$
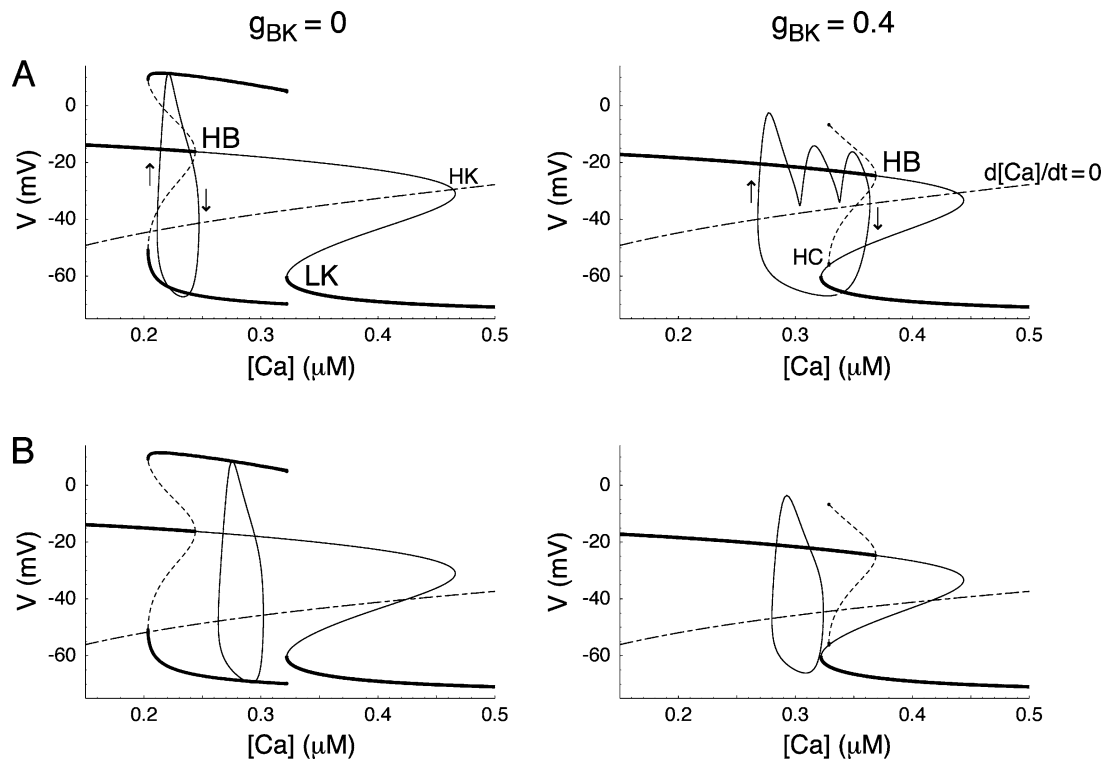
Fig. 3 Effects of I_{BK} on the fast subsystem bifurcation diagrams and the full system trajectory. A, $k_c = 0.16$ ms^{-1}. Increasing g_{BK} moves the periodic branch to the right and initiates bursting. Arrows indicate direction of motion. B, $k_c = 0.1$ ms^{-1}. The bifurcation diagrams are identical to A, but increasing g_{BK} does not lead to bursting and the trajectory moves only slightly to the right. In all panels, the z-shaped curve indicate the steady state of the system with [Ca] frozen (thick: stable; thin: unstable) and the ε-shaped curve indicate the minimum and maximum of periodic orbits (solid: stable; dashed: unstable). The dot-dashed curve is the [Ca]-nullcline. Above this curve $d[Ca]/dt > 0$ and below the curve $d[Ca]/dt < 0$. LK, low knee; HK, high knee; HB, Hopf bifurcation; HC, homoclinic bifurcation

with slow variations of [Ca] switching the system between the high and low steady states. [Ca] is only marginally slow to changes in voltage, so the trajectory overshoots the lower knee (LK) during the silent phase of bursting. Similarly, the trajectory leaves the stable portion of the upper branch prior to (in the case shown) the Hopf bifurcation (HB, where the upper steady state loses stability and an unstable limit cycle appears). Also, because [Ca] is not extremely slow, when the trajectory moves to the upper branch it does not have time to equilibrate to the stable spiral, and small oscillations are produced. These are the electrical impulses generated during the active phase of the cycle. This is a different picture than is found in many bursting cells, where bistability is between a low stationary branch and an upper periodic branch (Rinzel and Ermentrout, 1998).

Note that in principle, there could be bursting activity in the case shown in Fig. 3(A) left, because of the existence of a bistability region between a high steady state and the periodic branch (because the Hopf bifurcation is subcritical). If the [Ca]-nullcline were raised (i.e. for a higher value of the Ca^{2+} extrusion rate k_c) and [Ca] were slower, a bursting pattern would appear. However, this type of bursting, where activity alternates between spikes and damped oscillations at a depolarized level, is not observed in lactotrophs.

The LK of the z-curve is only slightly affected by the change in g_{BK} while the HB moves significantly to the right when g_{BK} is increased. Therefore, as g_{BK} is increased, the trajectory covers a larger range of [Ca] values, with the added range at higher [Ca] values. This means that the [Ca] fluctuations and the average [Ca] have increased. Thus, when g_{BK} is increased and the system is converted from spiking to bursting, the intracellular Ca^{2+} concentration is increased. This is also true, to a lesser extent, before the bursting regime is reached: as the periodic branch is slightly moved to the right by a small increase of g_{BK} over 0, the spiking trajectory is also moved to the right, thus [Ca] is increased (cf. Fig. 2(B)).

I_{BK} effects depend on Ca^{2+} dynamics

The effects discussed above are robust in the sense that regardless of the exact model parameters, increasing g_{BK} moves the periodic branch to the right, so for some value of g_{BK} a bistability region is created, bursting occurs and [Ca] is increased. However, details of this sequence of events may be altered, in part because [Ca] is not extremely slow.

Here, we change the parameter k_c that controls the rate of Ca^{2+} extrusion from the cell. If we decrease k_c the

Ca-nullcline moves down (cf. Eq. (3)) as shown on Fig. 3(B). Comparing the left panels of Fig. 3(A) and (B) ($g_{BK} = 0$) we see that this downward shift of the Ca-nullcline results in a shift of the trajectory to the right, i.e. the cell operates around a higher [Ca] value. This is expected since we have decreased the rate of Ca^{2+} extrusion. Now, when g_{BK} is increased, the trajectory moves only slightly to the right, since it starts from a position close to the low knee. In other words, for a smaller k_c value [Ca] does not rise as much with g_{BK}, since it is already elevated for $g_{BK} = 0$.

In addition, we see, on the right panel of Fig. 3(B), that increasing g_{BK} to 0.4 nS does not change the spike pattern to bursting as in Fig. 3(A). This is due to the lowering of the [Ca]-nullcline when k_c is decreased, so that $d[Ca]/dt$ is now larger during the upper part of the trajectory. As a result, [Ca] rises to a higher level during a spike and activates enough SK current to repolarize the membrane before a second spike can arise, preventing a burst from occuring. This behavior would not be expected from the fast/slow analysis, which assumes that [Ca] is a slowly changing variable. Indeed, slowing down the Ca^{2+} dynamics by decreasing f_c leads to bursting and increased [Ca]. Similarly, increasing g_{BK} further to widen the bistability range leads to bursting and increased [Ca] as in Fig. 3(A). Thus, the main result is the same: there is a transition from spiking to bursting and increased [Ca] when g_{BK} is increased sufficiently. This is shown on Fig. 4, which summarizes the previous results.

In Fig. 4(A), we plot the position (in terms of [Ca]) of the bifurcation points shown in Fig. 3, as g_{BK} is varied. As noted above, the high and low knees (HK and LK) of the z-curve are barely affected by g_{BK}. In contrast, the Hopf bifurcation (HB) and homoclinic bifurcation (HC, intersection of the periodic branch and middle branch of the z-curve) move to the right (i.e. to higher [Ca] values) as g_{BK} is increased. For g_{BK} above 0.2 nS, HB is on the right of LK, so a range of bistability exists and bursting is possible. Superimposed on this diagram are the ranges of variation of [Ca], for several g_{BK} values (solid: $k_c = 0.16$). The range of variation is greatly increased when the system is bursting rather than spiking. The mean of the variation is clearly right-shifted for higher g_{BK} values. Figure 4(B) is similar, but with trajectories (dashed) generated for $k_c = 0.1$. Bursting first occurs at a higher value of g_{BK} than with $k_c = 0.16$.

The average [Ca] as a function of g_{BK} is shown in Fig. 4(C). In both cases (solid: $k_c = 0.16$, dashed: $k_c = 0.1$) mean [Ca], $<Ca>$, increases with g_{BK}, but for $k_c = 0.1$ the increase is less extreme before the transition to bursting (arrows indicate where this transition occurs). In both cases, the main effect of increasing I_{BK} is to move the periodic branch to the right, which leads to bursting and higher $<Ca>$.
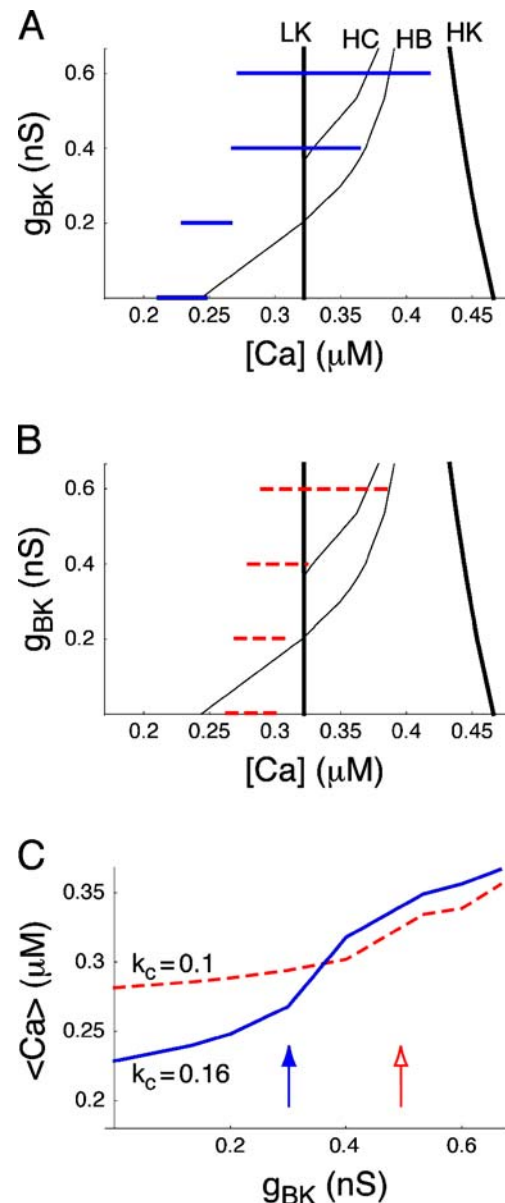
Fig. 4 Summary of the effects of I_{BK} on the lactotroph model. A, two-parameter bifurcation diagram. The diagram shows how the position of LK, HK, HB and HC (cf. Fig. 3) vary with g_{BK}. The main feature is that HB and HC move to the right when g_{BK} is increased, creating a region of bistability for $g_{BK} > 0.2$ nS. Horizontal bars represent the [Ca] variations during spiking or bursting of the model for various g_{BK} and $k_c = 0.16$. B, when k_c is reduced to 0.1 ms^{-1} bursting occurs at a higher value of g_{BK}. C, Effect of g_{BK} on the mean [Ca] for both values of k_c. Arrows indicate the onset of bursting (closed, blue: $k_c = 0.16$; open, red: $k_c = 0.1$ ms^{-1})

I_A converts spiking to bursting through different mechanisms

As for g_{BK}, increasing g_A transforms the spike pattern to bursting (Fig. 5). However, $<Ca>$ does not vary monotonically with g_A. Average [Ca] first increases following the transition to bursting at moderate g_A ($g_A = 8$ nS, Fig. 5(B))

Fig. 5 Effect of I_A on spike pattern, intracellular Ca^{2+} concentration and PRL release. A, $g_A = 0$, same as Fig. 2(A), showing the spiking regime and basal [Ca] and PRL levels. B, adding a small amount of A-type conductance ($g_A = 8$ nS) initiates bursting and increases [Ca] and PRL levels. C, a higher conductance ($g_A = 25$ nS) further increases burst duration but average [Ca] and PRL begin to decrease. In B and C, dotted lines represent the mean value, dashed lines represent mean value for $g_A = 0$
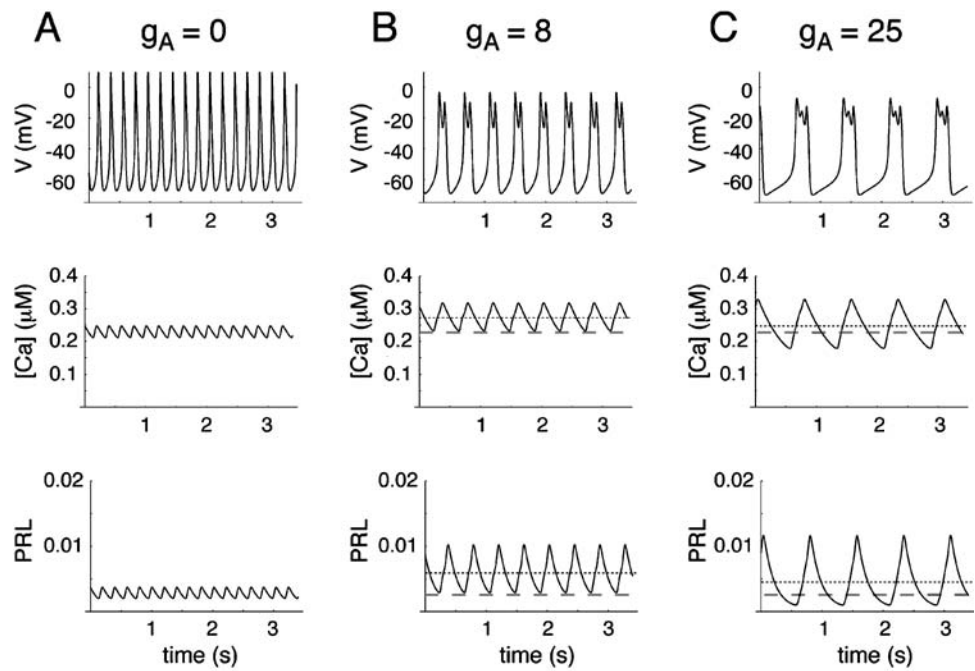
but then decreases for a higher value of the conductance ($g_A = 25$ nS, Fig. 5(C)), even though burst duration becomes longer. Hormone release (PRL) follows a pattern similar to [Ca], although the superlinear relationship between [Ca] and PRL release results in an amplification of the peak release. For this reason, while the mean [Ca] is only slightly increased for $g_A = 25$ nS relative to $g_A = 0$, the mean PRL is significantly increased.

To better understand how I_A affects the intracellular Ca^{2+} concentration we again use a fast/slow analysis. The fast subsystem is now 3-dimensional, with variables V, n and h (inactivation of I_A). Figure 6 reveals that I_A induces bursting differently than I_{BK}. We first consider the bifurcation diagrams of the fast subsystem shown in Fig. 6(A) for $g_A = 0$, 8 and 25 nS. The low knee (LK) moves leftward (i.e., lower [Ca]) as g_A is increased, while the position of the periodic
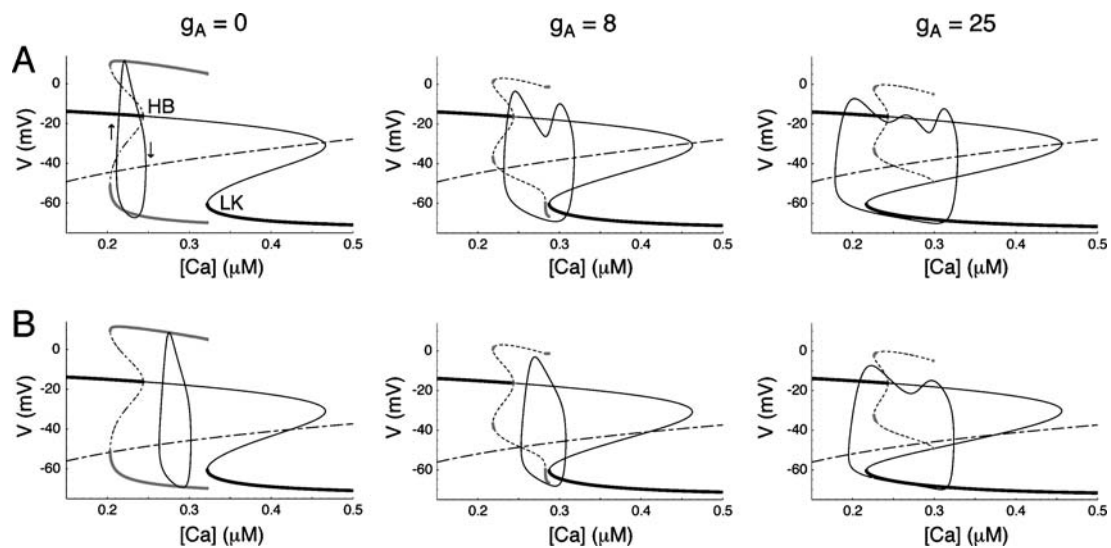
Fig. 6 Effects of I_A on the fast subsystem bifurcation diagrams and the full system trajectory. A, $k_c = 0.16$ ms^{-1}. Increasing g_A moves the low knee to the left, i.e. towards higher [Ca]. Left panel, spiking trajectory, same as Fig. 3(A) left. Middle panel, a bursting trajectory exists despite the lack of a bistability region between lower and upper branches. Most of the spiking branch is unstable. However, stable bursting and chaotic

solutions coexist with the unstable periodic branch (not shown). Right panel, the bursting trajectory encompasses (and slightly overshoots) the bistability region. B, $k_c = 0.1$ ms^{-1}. The bifurcation diagrams are identical to A, but the trajectories are restricted to narrower [Ca] ranges in the middle and right panels
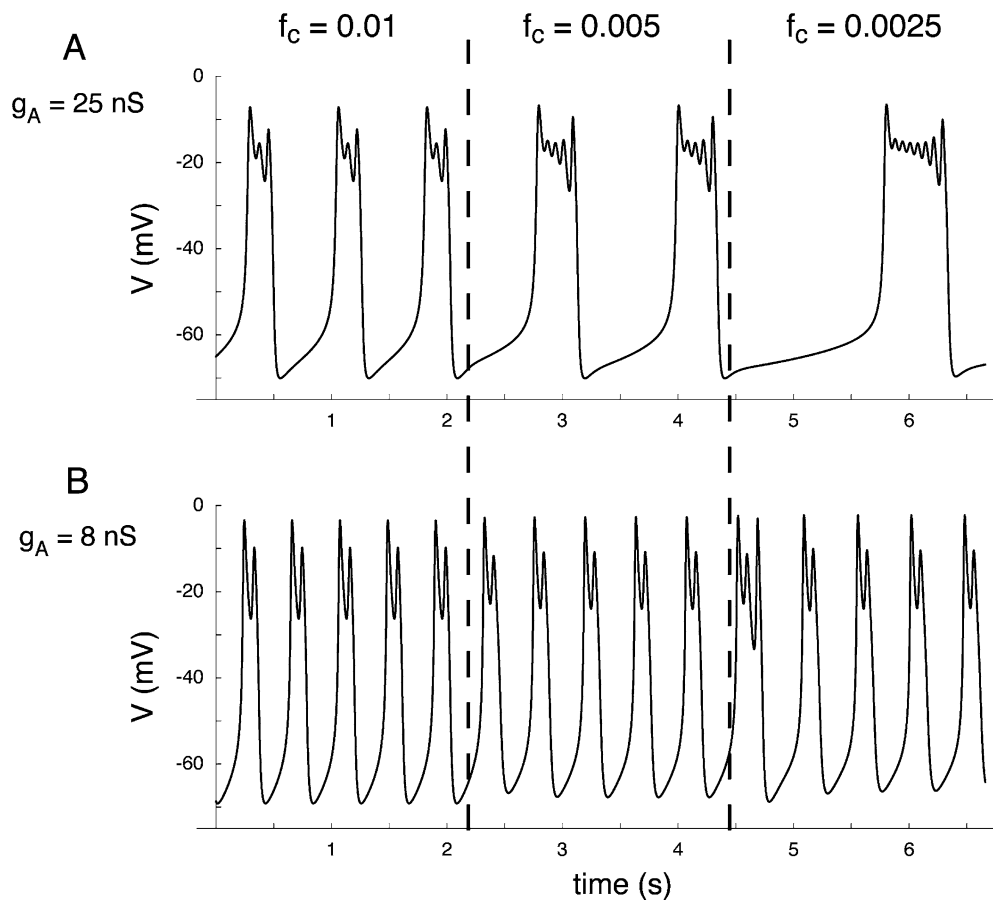
Fig. 7 Effect of increasing the [Ca] time constant on the bursting pattern. A, $g_A = 25$ nS, decreasing f_c slows down the bursts as expected for "classical" bursting. B, $g_A = 8$ nS, decreasing f_c has practically no effect on the burst pattern. The vertical dashed lines indicate the time when f_c was changed

branch is not affected. Consequently, a range of bistability is created (Fig. 6(A) right, $g_A = 25$ nS), and the full system trajectory cycles between the lower and upper branches.

I_A does not increase [Ca] monotonically as I_{BK} does, due to two important differences between the effects of I_A and I_{BK} on the fast subsystem. The first difference is that bursting can occur even if g_A is not large enough to create a region of bistability in the fast subsystem bifurcation digram. This is illustrated for $g_A = 8$ nS on Fig. 6(A). This bursting behavior occurs because the fast subsystem is intrinsically bursting. Although [Ca] varies and affects the bursting pattern, [Ca] dynamics are not necessary for bursting to occur in this case. Evidence for this is shown in Fig. 7. When $g_A = 25$ nS (Fig. 7(A)) increasing the time constant for [Ca] by decreasing f_c causes the bursting to slow down. This is expected if this bursting is driven by [Ca]. In contrast, when $g_A = 8$ nS (Fig. 7(B)) increasing the [Ca] time constant has little effect on bursting, indicating that [Ca] does not drive bursting in this case. Since all other variables (V, n, h) are fast relative to the burst period, we conclude that this bursting

behavior occurs in the absence of a slow variable. The mechanism for this latter type of bursting is examined in detail in Toporikova et al. (submitted). Here, we just note that the periodic "spiking" branch has become unstable (compare with $g_A = 0$) but a sequence of period doubling bifurcations occur as [Ca] is increased, creating branches corresponding to bursting and irregular (chaotic) oscillations (not shown). Finally, comparing with $g_A = 0$, we see that the spiking trajectory is extended by adding spike(s) "to the right", and thus the mean [Ca] is higher than for $g_A = 0$.

The second difference is that for larger g_A the region of bistability is created and extended by moving the low knee to the left, instead of moving the periodic branch to the right. Thus, as g_A is increased, new spikes are first added to the right of the trajectory $(g_A = 8$ nS), but for larger g_A new spikes are added to the left $(g_A = 25$ nS), i.e. at lower [Ca] values. This is unlike increasing g_{BK} which only adds spikes to the right. Thus, even though [Ca] fluctuations increase with g_A, the average [Ca] decreases once a region of bistability has been created.

I_A effects depend on Ca^{2+} dynamics

If the rate of Ca^{2+} extrusion, k_c, is reduced from 0.16 to 0.1 ms^{-1}, the [Ca]-nullcline is lowered and the effects of increasing g_A are slightly changed. Figure 6(B) shows that for $k_c = 0.1$ ms^{-1} and $g_A = 8$ nS (middle), the full system does not burst. Comparing with $g_A = 0$ nS (left), we see that the trajectory operates around similar [Ca] values, so for $k_c = 0.1$ ms^{-1} [Ca] levels do not change as g_A is increased
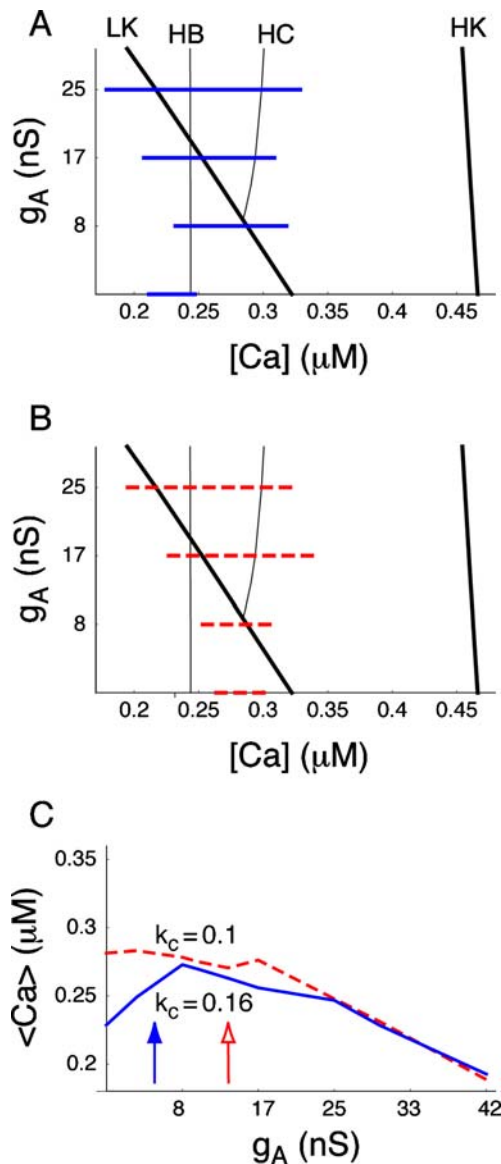
Fig. 8 Summary of the effects of I_A on the lactotroph model. A, two-parameter bifurcation diagram. As g_A is increased, the LK is moved to the left, creating a region of bistability for $g_A > 9$ nS. Horizontal bars represent the [Ca] variations during spiking or bursting for various g_A and $k_c = 0.16$. B, same for $k_c = 0.1$ ms^{-1}. C, Average [Ca] over a range of values of g_A. Arrows indicate the onset of bursting (closed, blue: $k_c = 0.16$; open, red: $k_c = 0.1$ ms^{-1}). For $k_c = 0.16$ < Ca > first increases with g_A and then decreases as a bistability range is created and the trajectory extends to lower [Ca] values

from 0 to 8 nS. As g_A is further increased (6(B), right) a region of bistability is created and the trajectory expands "to the left" so [Ca] levels decrease.

To summarize the effects of I_A, increasing g_A moves the low knee of the bifurcation diagram to the left and changes the stability of the periodic branch. At low g_A this may or may not lead to bursting accompanied by an increase in intracellular Ca^{2+}. As g_A is further increased, the movement to the left of the low knee creates a region of bistability and further g_A increase expands this region towards smaller [Ca] values. As a result, intracellular Ca^{2+} decreases. These results are summarized on Fig. 8.

Figures 8(A) and (B) illustrates that only the left knee (LK) of the fast subsystem bifurcation diagram is affected significantly by g_A. In 8(A) ($k_c = 0.16$ ms^{-1}), the horizontal bars that represent the range of [Ca] variations show that [Ca] first increases (range moves to the right) when g_A is increased to 8 nS, then slightly decreases (lower end of the range moves to the left in parallel to LK) for further increases in g_A. The corresponding variations of average [Ca] with g_A are shown on Fig. 8(C) (solid curve). In 8(B) (reduced Ca^{2+} extrusion rate, $k_c = 0.1$ ms^{-1}), the range of [Ca] variations (dashed horizontal lines) does not change very much when g_A is increased to 8 nS as there is no change in the spiking pattern. As g_A is increased further and the electrical activity becomes bursting, the lower end of the [Ca] range starts to move to the left. This decreases the average [Ca], as shown in 8(C) (dashed curve).

Discussion

In this study, we propose a mechanism for the stimulatory effect of a low dose of dopamine on prolactin secretion. The main hypothesis is that DA increases a fast K^+ current, which transforms the spiking pattern to bursting and increases Ca^{2+} influx. We showed that both I_{BK} (fast, non-inactivating) and I_A (fast, inactivating) could transform spiking into bursting, but through different mechanisms. Increasing I_{BK} always resulted in an increase in the mean intracellular Ca^{2+} concentration. Increasing I_A could also increase mean [Ca], but not in every case.

Assumptions and experimental tests

Much is known about how DA inhibits prolactin secretion by binding to D2 receptors (Ben-Jonathan and Hnasko, 2001). On the timescale of seconds, D2 receptor activation induces membrane hyperpolarization by opening inward rectifying K^+ channels (Gregerson et al., 2001). DA also increases the delayed rectifier and A-type K^+ currents (Lledo et al., 1990b), and possibly decreases Ca^{2+} conductances (Lledo et al., 1990a). This hyperpolarization prevents Ca^{2+} influx

through spiking, so [Ca] decreases and prolactin secretion is inhibited. On the other hand, the stimulatory effect of DA at low dose remains unexplained. Although this effect has been observed in several laboratories, there is contradictory evidence regarding the pathways involved in the stimulation of secretion. Some laboratories have shown that a D2 receptor subtype is involved (Burris et al., 1991; Chang and Shin, 1999), while others have proposed that D5 receptors may play a role in the stimulatory response (Porter et al., 1994). Similarly, a pertussis toxin sensitive G-protein pathway was suspected in one study (Tagawa et al., 1992) but had no effect in other studies (Burris et al., 1992; Chang et al., 1997).

If the stimulatory effect of DA is mediated by D2 receptors, it is likely that the pathways activated by a stimulatory concentration of DA form a subset of those activated by an inhibitory dose. Because a low DA concentration triggers Ca^{2+} influx within seconds (Burris and Freeman, 1993), it is reasonable to assume that this effect occurs by modulating ion channels. The known ionic currents affected by DA are the inward rectifier, delayed rectifier, BK and A-type K^+ currents (increased) and the Ca^{2+} currents (decreased). Activation of the inward rectifier hyperpolarizes the cell in a voltage-independent manner, incompatible with an increase in [Ca]. Similarly, an increase in the delayed rectifier K^+ current decreases [Ca]. In fact, our model simulations show that increasing the delayed rectifier conductance inhibits bursting while decreasing the delayed rectifier conductance can induce bursting with an increase in [Ca] (not shown). A decrease in Ca^{2+} currents is also unlikely to increase [Ca], because decreasing g_{Ca} would move the high knee of the bifurcation diagram (HK in Fig. 3) to the left, preventing bistability and thus bursting (not shown). Also, decreasing I_{Ca} would decrease Ca^{2+} influx for similar spike patterns. Therefore, the effect of DA most likely to quickly stimulate Ca^{2+} influx and prolactin release is an increase of either the fast BK current or the transient A-type current.

Our hypothesis, then, is that low concentrations of DA increase the conductance of either a BK or an A-type K^+ current, without affecting the inward rectifier. We propose that DA stimulates prolactin release through the transformation of spiking to a bursting pattern (or increase in burst duration) by these fast K^+ currents. Thus, only neurons that are spontaneously active will be stimulated by DA at low concentration. This is directly testable experimentally. Our hypothesis could be further tested by blocking one of these currents. If the blocked current is important in mediating the stimulatory effect of DA, then blocking the current should abolish this effect. In addition, we have assumed that the inward rectifier K^+ current is not activated by the low dose of DA required for stimulation. This current would, however, be activated at higher doses of DA. At intermediate concentrations between stimulatory and inhibitory, the excitatory effects of the fast K^+ currents would thus be counterbal-

anced by a small activation of the inward rectifier, so that there would be little effect of DA on [Ca] and PRL, compatible with experimental results (Burris and Freeman, 1993). Therefore, a further test of the model is that if the fast K^+ current is blocked, a dose of DA that normally has no effect on lactotrophs will be inhibitory. In practice, it is difficult to block individual K^+ currents since pharmacological blockers can have multiple effects. One approach would be to block all K^+ currents and then reintroduce specific currents using the dynamic clamp technique (Sharp et al., 1993).

We have assumed, for simplicity, that without dopamine both g_A and g_{BK} were null. This is probably not the case in most lactotrophs. Thus if DA increases one of these currents, it will be from a non-zero level. However, this does not qualitatively change the results presented here. Increasing I_{BK} moves the periodic branch of the bifurcation diagram to the right (Fig. 3), increasing the bistability range, regardless of the initial values of g_{BK} and g_A. Similarly, increasing I_A moves the low knee to the left (Fig. 6), increasing the bistability range to lower [Ca], regardless of the initial values of g_{BK} and g_A.

Because lactotrophs express g_A and g_{BK}, the present results illustrate that various amounts of these two conductances may lead to heterogeneous electrical properties in the lactotroph population. It has been proposed previously that lactotroph heterogeneity was due to differential expression of sodium or calcium channels (Horta et al., 1991; Lledo et al., 1991). These differences in expression of the inward currents would separate lactotrophs into active and silent subpopulations. In addition, heterogeneity of the fast K^+ channels could further subdivide the active population into spikers and bursters. Finally, we showed that Ca^{2+} dynamics could also play a role in dividing lactotroph cells between spikers and bursters. Decreasing the extrusion rate k_c could prevent bursting because [Ca] is not an extremely slow variable in our model. However, slowing down [Ca] by decreasing the fraction of free cytosolic Ca^{2+} (f_c) could switch the spike pattern back to bursting in that case (not shown), as was recently shown for cerebellar granule cells (Roussel et al., 2006).

Different mechanisms for switching from spiking to bursting

We have deliberately chosen a simplified model to investigate the role of the fast K^+ currents. The model of Van Goor et al. (2001a) incorporated two Ca^{2+} channels (L and T) and multiple Ca^{2+} compartments to simulate spatial heterogeneity of Ca^{2+} concentration and its effect on SK and BK channels. Their model of the BK current included the dependence on both membrane voltage and Ca^{2+} concentration in the vicinity of the channels (the "domain" Ca^{2+}). Here we have simply used a fast voltage-dependent conductance to model the BK channels, justified by the parallel time courses

of voltage and domain Ca^{2+} observed by Van Goor et al. (2001a, Fig. 11(B)). The simplicity of our model has allowed us to perform a fast/slow analysis and reveal that I_{BK} and I_A can affect the electrical activity of the lactotrophs through superficially similar, but distinct, mechanisms. These mechanisms are general, in the sense that they do not depend on precise parameter values for the current kinetics.

I_{BK} transforms the spike pattern to bursting by moving the periodic branch to the right. This is because adding or increasing I_{BK}, a fast K^+ current, is similar to making the delayed rectifier K^+ current (I_K) faster. This can be done directly by increasing the parameter λ in Eq. (2) (Bertram et al., 1995). Speeding up activation of I_K decreases the delay between the positive feedback provided by the Ca^{2+} current and the negative feedback provided by I_K. If this delay is too small, oscillations do not occur, the unstable steady states on the upper branch in Fig. 3(A) (left) become stable. In other words, the Hopf bifurcation is moved to the right, as occurred when g_{BK} was increased. Thus, adding I_{BK} in our model is similar to speeding up the fast negative feedback (I_K). The result is that a region of bistability between upper and lower steady states is created and extended to the right, towards higher [Ca]. This is how I_{BK} transforms the spike pattern to bursting and increases [Ca]. This mechanism does not depend on the exact kinetics of I_{BK}, as long as I_{BK} is fast compared to I_K.

The mode of action of I_A is very different. Activation of this current occurs at a much lower voltage than I_K (cf. Fig. 1). Because of this, it takes less activation of the Ca^{2+}-dependent K^+ current (I_{SK}), and thus less [Ca], to maintain the cell at a resting state. Therefore, increasing g_A moves the low knee of the bifurcation diagram to the left (Fig. 6). This also creates and extends a region of bistability, but this extension is made at lower [Ca]. Thus, when the bistability region is created, higher g_A yields longer bursts but also lowers the average [Ca]. Finally, I_A affects the stability of the periodic branch, but not its location. It does this by inducing a sequence of period doubling bifurcations, as was observed in other models of excitable cells that incorporated an inactivating K^+ current (Doiron et al., 2002; Rush and Rinzel, 1995). Bursting solutions can be created from these period doubling bifurcations, at fixed [Ca] values. Thus, I_A can induce intrinsic bursting of the fast subsystem, that is, bursting without the classical combination of a slow variable and a region of bistability (Toporikova et al., submitted). This mechanism is important, since it leads to an increase in the mean Ca^{2+} concentration.

Conclusion

The fast K^+ currents (I_A and I_{BK}) can change the electrical activity in a lactotroph model from spiking to bursting.

This change may be associated with an increase in intracellular Ca^{2+} concentration, increasing the level of hormone release. Increase of one of these currents by DA may thus be the mechanism for the stimulatory effect of DA at low concentration.

References

Arey BJ, Burris TP, Basco P, Freeman ME (1993) Infusion of dopamine at low concentrations stimulates the release of prolactin from Alpha-Methyl-P-Tyrosine-treated rats. Proc. Soc. Exp. Biol. Med. 203: 60–63.

Ben Jonathan N, Hnasko R (2001) Dopamine as a prolactin (PRL) inhibitor. Endocr. Rev. 22: 724–763.

Bertram R, Butte MJ, Kiemel T, Sherman A (1995) Topological and phenomenological classification of bursting oscillations. Bull. Math. Biol. 57: 413–439.

Burris TP, Freeman ME (1993) Low concentrations of dopamine increase cytosolic calcium in lactotrophs. Endocrinol. 133: 63–68.

Burris TP, Nguyen DN, Smith SG, Freeman ME (1992) The stimulatory and inhibitory effects of dopamine on prolactin secretion involve different G-Proteins. Endocrinol. 130: 926–932.

Burris TP, Stringer LC, Freeman ME (1991) Pharmacological evidence that a D2-Receptor subtype mediates dopaminergic stimulation of prolactin secretion from the anterior-pituitary gland. Neuroendocrinol. 54: 175–183.

Chang A, Shin SH (1999) Dopamine agonists both stimulate and inhibit prolactin release in GH(4)ZR(7) cells. Eur. J. Endocrinol. 141: 387–395.

Chang A, Shin SH, Pang SC (1997) Dopamine D-2 receptor mediates both inhibitory and stimulatory actions on prolactin release. Endocrine 7: 177–182.

Chay TR, Keizer J (1983) Minimal model for membrane oscillations in the pancreatic beta-cell. Biophys. J. 42: 181–189.

Denef C, Manet D, Dewals R (1980) Dopaminergic stimulation of prolactin-release. Nature 285: 243–246.

Dodge FA, Rahamimoff R (1967) Co-operative action of calcium ions in transmitter release at neuromuscular junction. J. Physiol. Lond. 193: 419–432.

Doiron B, Laing C, Longtin A, Maler L (2002) Ghostbursting: A novel neuronal burst mechanism. J. Comput. Neurosci. 12: 5–25.

Einhorn LC, Gregerson KA, Oxford GS (1991) D2 dopamine receptor activation of potassium channels in identified rat lactotrophs—whole-cell and single-channel recording. J. Neurosci. 11: 3727–3737.

Ermentrout B (2002) Simulating, analyzing, and animating dynamical systems SIAM.

Gregerson KA, Flagg TP, O'Neill TJ, Anderson M, Lauring O, Horel JS, Welling PA (2001) Identification of G protein-coupled, inward rectifier potassium channel gene products from the rat anterior pituitary gland. Endocrinol. 142: 2820–2832.

Helmchen F, Imoto K, Sakmann B (1996) Ca^{2+} buffering and action potential-evoked Ca^{2+} signaling in dendrites of pyramidal neurons. Biophys. J. 70: 1069–1081.

Herrington J, Lingle CJ (1994) Multiple components of voltage-dependent potassium current in normal rat anterior-pituitary-cells. J. Neurophys. 72: 719–729.

Horta J, Hiriart M, Cota G (1991) Differential expression of Na channels in functional subpopulations of rat lactotropes. Am. J. Physiol. 261: C865–C871.

Kanyicska B, Freeman ME, Dryer SE (1997) Endothelin activates large-conductance K$^+$ channels in rat lactotrophs: Reversal by long-term exposure to dopamine agonist. Endocrinol. 138: 3141–3153.

Liu LX, Shen RY, Kapatos G, Chiodo LA (1994) Dopamine neuron membrane physiology—characterization of the transient outward current (I-A) and demonstration of a common signal-transduction pathway for I-A and I-K. Synapse 17: 230–240.

Lledo PM, Guerineau N, Mollard P, Vincent JD, Israel JM (1991) Physiological characterization of 2 functional-states in subpopulations of prolactin cells from lactating rats. J. Physiol.- Lond. 437: 477–494.

Lledo PM, Legendre P, Israel JM, Vincent JD (1990a) Dopamine inhibits 2 characterized voltage-dependent calcium currents in identified rat lactotroph cells. Endocrinol. 127: 990–1001.

Lledo PM, Legendre P, Zhang J, Israel JM, Vincent JD (1990b) Effects of dopamine on voltage-dependent potassium currents in identified rat lactotroph cells. Neuroendocrinology 52: 545–555.

Neher E, Augustine GJ (1992) Calcium gradients and buffers in bovine chromaffin cells. J. Physiol. Lond. 450: 273–301.

Oxford GS, Tse A (1993) Modulation of ion channels underlying excitation-secretion coupling in identified lactotrophs and gonadotrophs. Biol. Reprod. 48: 1–7.

Porter TE, Grandy D, Bunzow J, Wiles CD, Civelli O, Frawley LS (1994) Evidence that stimulatory dopamine-receptors may be involved in the regulation of prolactin secretion. Endocrinol. 134: 1263–1268.

Prakriya M, Lingle CJ (2000) Activation of BK channels in rat chromaffin cells requires summation of Ca^{2+} influx from multiple Ca^{2+} channels. J. Neurophysiol. 84: 1123–1135.

Rinzel J, Ermentrout GB (1998) Analysis of neural excitability and oscillations. In: C Koch, I Segev, eds. Methods in Neuronal Modeling. MIT Press, Cambridge.

Roberts WM, Jacobs RA, Hudspeth AJ (1990) Colocalization of ion channels involved in frequency-selectivity and synaptic transmission at presynaptic active zones of hair-cells. J. Neurosci. 10: 3664–3684.

Roussel C, Erneux T, Schiffmann SN, Gall D (2006) Modulation of neuronal excitability by intracellular calcium buffering: From spiking to bursting. Cell Calcium 39: 455–466.

Rush ME, Rinzel J (1995) The potassium A-current, low firing rates and rebound excitation in hodgkin-huxley models. Bull. Math. Biol. 57: 899–929.

Sharp AA, Oneil MB, Abbott LF, Marder E (1993) Dynamic clamp—Computer-generated conductances in real neurons. J. Neurophysiol. 69: 992–995.

Tagawa R, Takahara J, Sato M, Niimi M, Murao K, Ishida T (1992) Stimulatory effects of quinpirole hydrochloride, D2-dopamine receptor agonist, at low concentrations on prolactin-release in female rats *invitro*. Life Sci. 51: 727–732.

Van Goor F, Li YX, Stojilkovic SS (2001a) Paradoxical role of large-conductance calcium-activated K$^+$ (BK) channels in controlling action potential-driven Ca^{2+} entry in anterior pituitary cells. J. Neurosci. 21: 5902–5915.

Van Goor F, Zivadinovic D, Martinez-Fuentes AJ, Stojilkovic SS (2001b) Dependence of pituitary hormone secretion on the pattern of spontaneus voltage-gated calcium influx—Cell type-specific action potential secretion coupling. J. Biol. Chem. 276: 33840–33846.

Van Goor F, Zivadinovic D, Stojilkovic SS (2001c) Differential expression of ionic channels in rat anterior pituitary cells. Mol. Endocrinol. 15: 1222–1236.